Absolute Measurements of Ultrasonic Pressure by Using High Magnetic Fields

Yehuda Sharf, Greg T. Clement, and Kullervo Hynynen, *Member, IEEE*

***Abstract*—A hydrophone is introduced that exploits the emf signal generated in a conductor when sonicated in the presence of a uniform static magnetic field. The method uses a small metal coil or metal membrane as a hydrophone receiver. Acoustic signals at 748 kHz are introduced in 1.5T and 4.7T fields and recorded both through direct electrical contact with the hydrophone and via RF pick-up coils, allowing wireless placement of the hydrophone. Linear response is confirmed over four orders of magnitude in the pressure amplitude. Waveforms determined from the detected voltage are shown to be in excellent agreement with those obtained using a calibrated polyvinylidene difluoride film, and absolute values correlate within 20%. The methods are conceptually suitable for use in the presence of the high and uniform field of commercial MR scanners. The hydrophone may appear particularly useful as a quality assurance device in therapeutic and diagnostic acoustic techniques that use MRI.**

I. Introduction

It is well established that a transverse voltage is induced in conducting metals sonicated in the presence of a magnetic field [1]. This magnetoacoustic interaction has been used for numerous applications, including the design of electrodynamic transducers [2],[3]. Previously reported transducers have relied on the presence of a sharp magnetic field gradient to produce an electric signal. These transducers involve a conducting coil oriented such that the magnetic field is appreciable only along one side of the coil. Acoustic displacement of the coil then results in a net electric potential as dictated by the Lorentz force. In the present study we introduce a hydrophone that allows the measurement of an ultrasound signal in a strong uniform magnetic source, such as the field provided by an MRI scanner. The hydrophone uses a small wire coil positioned normal to the axis of acoustic propagation as a detector. The voltage at the coil leads is shown to be linearly proportional to the acoustic pressure. Additionally the induced electric signal generates a radiating field, suggesting wireless transmission is possible when the hydrophone is used in conjunction with RF pick-up coils.

By operating through a static magnetic field, the hydrophone may hold utility in ultrasound applications used in conjunction with MRI. An apt example is MR-guided focused ultrasound surgery [4], an ultrasound hyperthermia procedure that uses MRI to steer an ultrasound beam while monitoring thermal dosage. The application would exploit the coil's durability and accuracy at high amplitudes. The hydrophone could provide immediate information on waveform shape and magnitude at intensities not accessible to most receivers. A marked advantage would be the ability to obtain absolute measurements of the pressure amplitude, a quantity necessary for calculation of thermal energy transfer.

The coil hydrophone design is based on a variation of an electromagnetic (EM) hydrophone originally proposed by L. Filipczynski [2]. The original design operates in the gradient of a permanent magnet. Our design, described theoretically in Section II, uses a rectangular coil wrapped about an electrically insulating core to obtain a net signal in a uniform field. An acoustic signal is passed through the coil, so the axis of acoustic propagation is perpendicular to the coil's axis. Use of a long coil dimension in the direction of the acoustic propagation makes it possible to separate the entering and exiting signal. Theoretical development predicts the coil to yield a rather broadband and flat response. A typical -3 dB bandwidth ranges from DC to an upper frequency determined by the wire diameter, generally in the range of 1-10 MHz. This response is tested using the procedures described in Section II. Time history and amplitude measurements, presented in Section III,A, are found to be in excellent agreement with a commercial PVDF hydrophone over a broad range of frequencies and amplitudes. Results suggest application of the hydrophone as a transducer calibration method.

To demonstrate the feasibility of wireless measurement, RF pick-up coils described in Section III,B are used to record the time trace of an ultrasound pulse directed through metal foils. Results are described in Section III,B. These time-dependent potentials are shown to exhibit strong correlation with the time traces of the acoustic pressure measured with a polyvinylidene difluoride (PVDF) hydrophone.

II. Theoretical Background

An acoustic pulse is considered in the presence of a magnetic field. According to the flux rule for motion in a static magnetic field, a conducting coil consisting of N-

Manuscript received December 31, 1998; accepted June 11, 1999. Support for this study was provided in part by the Rothschild Foundation. This research was also supported by Grant No. CA 46627 from the National Institutes of Health.

The authors are with Department of Radiology, Brigham and Women's Hospital, Harvard Medical School, 221 Longwood Ave., Boston, MA 02115 (e-mail: clement@bwh.harvard.edu).

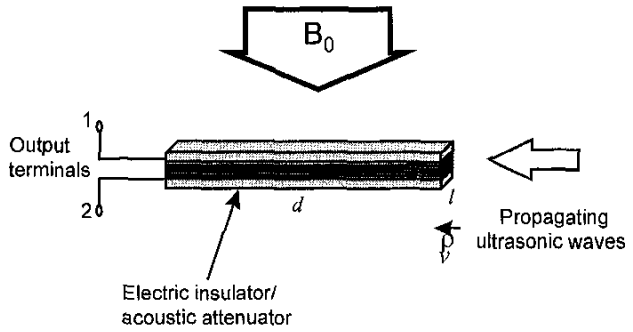

Fig. 1. The coil hydrophone. An electromotive force is induced in the segments perpendicular to the propagation axis and the magnetic field. The electric insulator absorbs ultrasonic pressure over the length of the coil, d. The 6-turn coil tested has dimensions $d = 40$ mm $\times\, l = 3.2$ mm. The height across the six turns is 0.7 mm.

turns, placed in the path of propagation will experience an electromotive force (emf) of:

$$V = -N\frac{d}{dt}\oint \mathbf{B}\cdot\mathbf{n}dA \tag{1}$$

across its terminals. The relevant case involves a rectangular coil placed in a static magnetic field normal to the acoustic axis of propagation (Fig. 1). The emf under this geometry experiences a time-variation proportional to the sound-induced area change of the coil. In terms of the particle displacement velocity in the conductor, v, (1) reduces to:

$$V(t) = -NB_0\oint v(\mathbf{r},t)dr, \tag{2}$$

where the path of integration is taken about the rectangular coil. In the present case all sides of the rectangular coil experience the same magnetic field. Thus, both the near and far sides of the coil relative to the transducer contribute to the integral in (2). These contributions can be constructive or destructive depending on the dimensions of the coil and the ultrasonic wavelength, λ, inside the electric insulator. This ambiguity may introduce complications in the analysis of the signal. However, these complications can be circumvented by increasing the depth of the coil, making it much longer than the ultrasonic pulse length. If required, an electric insulator with high acoustic attenuating properties may be used as the core of the coil. Lengthening the coil simply separates the signals of the near and far sides of the coil while attenuation reduces the ultrasonic pressure and, accordingly, the vibrations of the conductor along the far side.

The face of the hydrophone manifests a three layer system, where the mechanical impedances of the liquid, the conductive layer and the insulator, are given by Z_l, Z_i, and Z_c, respectively. The ratio between the absolute pressure amplitude of the penetrating wave p_i and incident wave p_l is given by [5]:

$$\frac{|p_i|}{|p_l|} = \left|\left[\frac{Z_i+Z_l}{2Z_i}\cos\left(\frac{2\pi f l_c}{C}\right) + j\frac{Z_c^2+Z_iZ_l}{2Z_iZ_c}\sin\left(\frac{2\pi f l_c}{c}\right)\right]^{-1}\right| \tag{3}$$

where l_c is the thickness of the conductive layer, f is the frequency, and c is the velocity of the longitudinal wave in the conductor. The equation is valid for incident planar waves which requires that the receiving face be small relative to variation in the acoustic beam geometry.

A thin conductive layer is considered with a thickness small relative to the acoustic wavelength, $l_c \ll \lambda$. For most conductive metals at ultrasonic frequencies of less than 10 MHz, this implies layer thickness of less than 10 μm. It is further assumed that the mechanical impedance of the conductor is much higher than that of both the liquid and the insulator assuring the condition $Z_c^2 \gg Z_l^2, Z_i^2, Z_lZ_i$ is satisfied. Under these assumptions, the amplitude ratio in (3) can be approximated to second order by:

$$\frac{|p_i|}{|p_l|} \cong \frac{2Z_i}{Z_i+Z_l}\left\{1-\left[\frac{\sqrt{2}\pi f l_c Z_c}{c(Z_i+Z_l)}\right]^2\right\}. \tag{4}$$

The particle velocity can then be calculated accordingly:

$$v = \frac{p_i}{Z_i} \cong \frac{2p_l}{Z_i+Z_l}\left\{1-\left[\frac{\sqrt{2}\pi f l_c Z_c}{c(Z_i+Z_l)}\right]^2\right\}. \tag{5}$$

Substitution of the solution to (5) into (2) allows the pressure amplitude of a plane wave propagating in the liquid to be evaluated directly from the detected voltage:

$$P_l \cong \frac{V(Z_l+Z_i)}{2B_0Nl}\left\{1-\left[\frac{\sqrt{2}\pi f l_c Z_c}{c(Z_i+Z_l)}\right]^2\right\}^{-1}. \tag{6}$$

It is evident from this expression that thin conducting layers, in practice of the order of 1-5 μm, exhibit a flat and wide band frequency response. As the layer thickness increases, there is a sharp decrease in the signal intensity with frequency [2]. However, as long as the thin layer approximation is valid, (6) provides a correction for the pressure amplitude estimation. To implement (5) in case of a cylindrical wire, the mean displacement across the wire due to varying thickness must be calculated. This averaging represents only an approximation to the wire's overall contribution. In (6), as the wire becomes very thin, the thickness term may be neglected altogether. The value is obtained by integrating across the wire,

$$\langle v(l)\rangle = \frac{2p_l}{Z_i+Z_l}\frac{1}{2R}\int_{-R}^{R}\left\{1-\left[\frac{2\sqrt{2}\pi f Z_c\sqrt{R^2+l^2}}{c(Z_i+Z_l)}\right]^2\right\}dl, \tag{7}$$

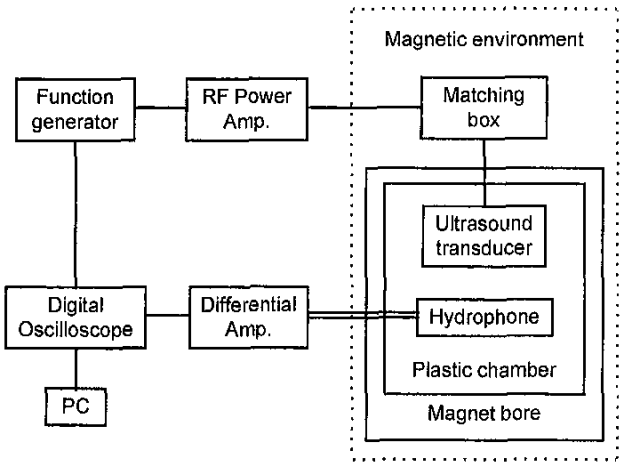

Fig. 2. A schematic block diagram of the experimental apparatus.

where R is the wire radius and the thickness is given by $l_c = 2\sqrt{R^2 - l^2}$. The solution of (7),

$$\langle v \rangle = \frac{2p_l}{Z_i + Z_l}\left\{1 - \frac{16}{3}\left[\frac{\pi f Z_c R}{c(Z_i + Z_l)}\right]^2\right\} \tag{8}$$

may be substituted into (2) to yield a result similar to (6) with the substitution $l_c \Rightarrow \sqrt{\frac{8}{3}}R$.

III. Materials and Methods

A. Measurements in the Magnetic Field

A schematic diagram of the experimental setup for the measurement of the ultrasonic field inside the magnet is given in Fig. 2. The transmission lines as well as most of the detection circuitry were identical for all measurements. A single element 0.748 MHz air-backed focused ultrasound transducer was used. Its diameter and radius of curvature were 40 mm and 100 mm, respectively. The transducer was matched to a 50Ω impedance at its working frequency. The matching circuit was shielded and was physically located about 1.5 m from the opening of the magnetic bore. A 100 MHz synthesized arbitrary waveform generator (Wavetek model 395) was used to generate input signals to a 55 dB 0.3 -33 MHz RF power amplifier (ENI model A150).

Measurements were conducted in two different magnetic fields: 1.5 T (manufactured in-house) and 4.7 T (Oxford Instruments model A25776). Magnet bore sizes were 60 cm and 20 cm, respectively. All measurements were performed in a cylindrical plastic chamber illustrated in Fig. 3(a). The hydrophone coil illustrated in Fig. 1 was fixed to an open-ended cylindrical plastic hydrophone holder (57.4 mm OD; 50.6 mm ID) that was free to slide up and down along a cylindrical water tank 70 mm ID and 150 mm in height. The coil axis aligned parallel with magnetic field vector. The ultrasound transducer was fixed to a 2 mm thick rubber layer and placed facing up on the floor of the chamber.

The dual coax detection lines fed a differential amplifier (Preamble Instrument model 1820). The input resistance was set to 1MΩ and a hi-pass filter of >10 kHz was used. The signal was sampled using 50Ω input HP 54510A 250 MHz 1 GSa/s digitizing oscilloscope and transferred to a portable PC using GPIB ports. When the input voltage saturated the scope due to transmission line coupling, a logical analog switch driven by another pulse generator was used to gate the input.

B. Hydrophone Coil

The rectangular coil hydrophone used in our experiments is illustrated in Fig. 3(a). It consists of six turns of a 38 AWG 0.008 mm^2 Belden magnet wire around a Plexiglass core. All measurements were performed in a cylindrical plastic chamber. The minimum bore size restricted the dimensions of the chamber to 70 mm ID and 150 mm of height. The ultrasound applicator was fixed to a 2 mm thick rubber layer and placed facing up on the floor of the chamber. The dimensions of the receiving face of the coil were 3.2 mm × 0.7 mm. Because the acoustic velocity inside the plastic is about 2600 m/s, the length of the plastic block of 40 mm is more than 11 times the ultrasonic wavelength of about 3.5 mm. The attenuation coefficient of the plastic core is approximately 2 dB/cm-MHz [6].

For the calculation of the pressure amplitude the characteristic impedance of water (1.5×10^6 Pa s/m), plastic (3.2×10^6 Pa s/m), and copper (42×10^6 Pa s/m) were applied to (7). Using these values and assuming the wire radius to be a constant value of 51 μm and the velocity of sound inside the copper wire is 4700 m/s [3], the calibration relation between the pressure amplitude and the potential across the coil is given by:

$$P = \alpha\frac{V}{B_0},$$

$$\alpha = \frac{Z_l + Z_i}{2Nl}\left\{1 - \frac{16}{3}\left[\frac{\pi f R Z_c}{c(Z_i + Z_l)}\right]^2\right\}^{-1} \tag{9}$$

with $\alpha = 1.69 \times 10^8$ T · Pa/V for a given field B_0 at the transducer resonant frequency of 0.748 MHz. The detected voltage V is given in volts, B_0 in Teslas, and the pressure amplitude in Pascals. The hydrophone calibration constant α is seen in Fig. 4(a) to vary slowly at frequencies below 1 MHz, exhibiting a −6 dB bandwidth of DC to 1.0 MHz. For the study of submegahertz waves, the wire yields less than 10% deviation in the measured field. However, measurements at higher frequencies (>1 MHz) would require the use of thinner wire. For example, a 6-turn coil similar to that described here but wound with 5 μm wire would produce a substantial bandwidth increase (DC to 10.2 MHz, −6 dB), as indicated in Fig. 4(b).

Ultrasonic field measurements outside the magnet were carried out in degassed water using a needle type 1.0 mm PVDF hydrophone (Precision Acoustic LTD) equipped

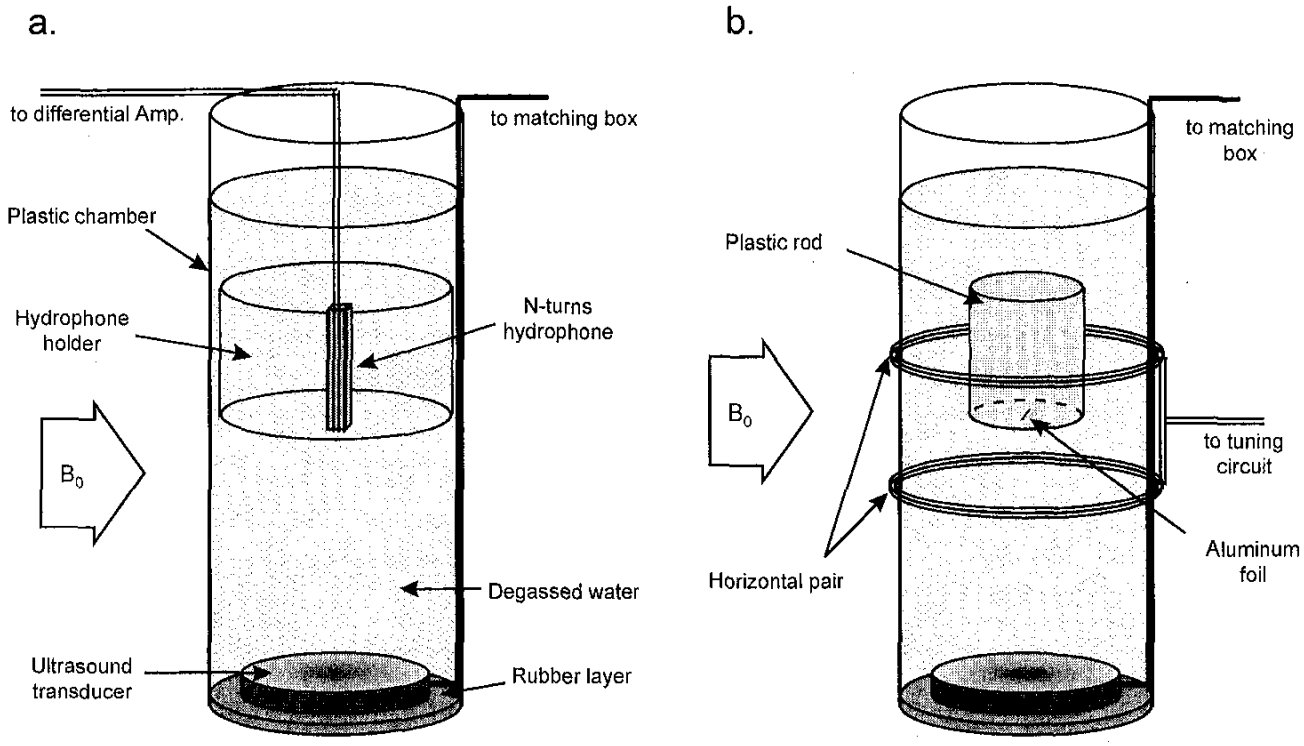

Fig. 3. The experimental setup for testing hydrophones inside the magnet. Ultrasound waves propagate perpendicular to magnetic fields B_0. The cylindrical plastic hydrophone holder is 50.6 mm ID, and the cylindrical water tank 70 mm ID and 150 mm in height. The transducer is fixed on 2-mm thick rubber. In (a) the terminals of the hydrophone are connected to the differential amplifier. In (b) the horizontal coils pick up the RF signal generated by the oscillating electrons in the vibrating conductive element. The coils are connected through a tuning circuit to the differential amplifier.

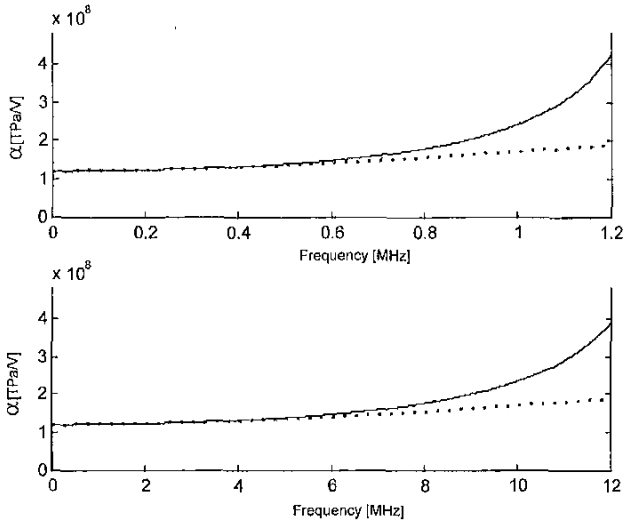

Fig. 4. Frequency dependence of the coil hydrophone calibration constant. The top graph shows values for a 51 μm-radius wire using the thin wire approximation given by (4) (solid) and without the approximation (dashed). Below, similar calculation for a 5 μm-radius wire reveals linearity across an increased bandwidth.

with a submersible preamplifier and a DC coupler (Precision Acoustic LTD). To obtain an independent and absolute assessment of the pressure field, the calibration factor was determined using the method described by Herman and Harris [7]. The total acoustic power of the 0.748 MHz transducer was obtained from a radiation force measuring device using an absorbing target. The same field was then scanned in a plane at the focus with the PVDF hydrophone. The recorded potential is related to the total power by the factor:

$$\beta = \sqrt{\frac{P_T}{Z_w \iint V(r)dA}}. \tag{10}$$

Assuming no loss through the media of degassed water, this procedure yielded a calibration factor of $\beta = 1824$ nV/Pa.

C. RF Pickup Coils

For the wireless reception demonstration, two pairs of RF pickup coils, one horizontal and one vertical, were used. The coils were mounted on an outer plastic cylinder of larger diameter (76.4 mm OD; 69.8 mm ID) and could be adjusted to the desired position. Each pair included two identical 15-turn coils. The horizontal pair is illustrated in Fig. 3(b). One end of each coil was connected to ground;

the other terminals were connected through a tuning circuit to the input of the differential amplifier. The vertical pair could be positioned with its axis at an arbitrary angle perpendicular to the axis of sonication. The diameter of each vertical coil was 64 mm, and the gap between the two coils was 83 mm. The horizontal pair was placed with its axis coinciding with the axis of sonication. Here, the gap between the two coils was 23 mm, and their diameter was 76.4 mm. Prior to measurements, the coils were tuned to the corresponding ultrasonic transducer frequency. The Q value of the receiving coils could be set using a resistor across the two coils. In place of the hydrophone coil, a solid conductive element was used. The element was made of a 20 μm thick aluminum foil mounted, as shown in Fig. 3(b), on a 40 mm long cylindrical Plexiglas rod ($d = 25$ mm).

A strong coupling signal between the RF coils and the ultrasonic transmission appeared at zero field outside the magnet. This RF coupling noise was highly reduced by the differential amplifier; however, its level remained relatively high. The noise level was further reduced when the bottom part of the chamber was shielded. However, high pressure fields caused the amplified coupling signal to exceed the maximum allowed overdrive input of 100 V and saturated the scope. This problem was solved using an analog switch that gated the input to the scope and allowed the RF interference from the transducer to be separated from the signal received by the hydrophone. Another source of noise appeared only in the 4.7 Tesla magnet inside the magnet and was identified with the interference with the MR shim coils. This noise was eliminated by fixing additional shielding or simply by turning off the supply to the shim coils.

IV. Results and Discussion

A. Coil Hydrophone

The six-turn hydrophone coil was positioned in the 1.5 T magnetic field along the center of the ultrasonic beam and perpendicular to the sonication axis [Fig. 3(a)]. The active element of the detector was located 100 ± 1 mm from the center of the transducer. Burst lengths of 1, 4, and 10 cycles were input to the transducer, and the coil response was recorded. The maximum peak-to-peak signal measured as a function of the input voltage is displayed in Fig. 5. The field was measured over the full amplitude range of the driving amplifier. The lower threshold for signal detection is determined by detection of the signal above background noise. Because sensitivity of the signal is linearly proportional to the magnetic field strength, a stronger magnet would allow a weaker signal to be detected. For the 4.7 T magnet, a background noise was observed on the order of 1.5 μV rms over 64 averages, which would allow the detection of signals slightly below 1 kPa. Identical signals were recorded outside the magnet using the PVDF hydrophone tip, also positioned on the axis of propagation 100 mm from the transducer surface. Time traces for comparing the PVDF and the coil hydrophone are presented in Fig. 6, showing excellent agreement.

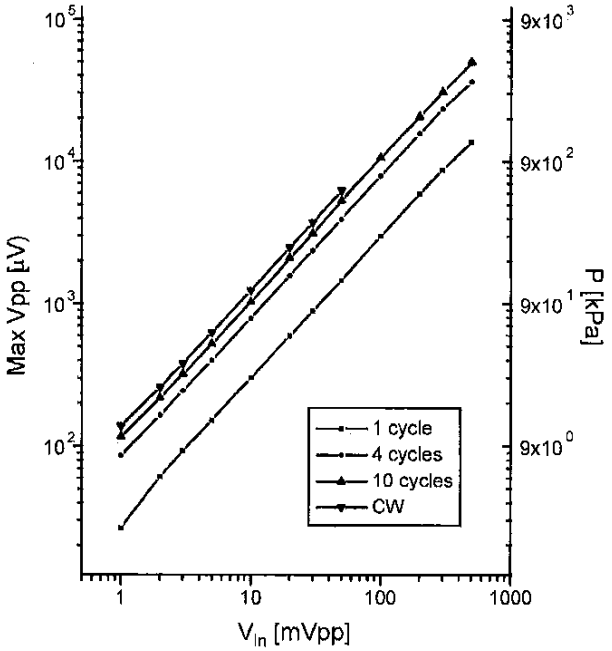

Fig. 5. A graph of the output voltage and the corresponding pressure amplitude measured using the 6-turn hydrophone as a function of voltage input to a 55 dB amplifier. The four lines correspond to burst lengths of 1, 4, and 10 cycles as well as for CW. These measurements were carried inside the 4.7 T magnet.

The pressure amplitude then was measured as a function of distance from the transducer. This was accomplished by sliding the coil in 5 mm steps along the chamber. Again measurements were conducted for burst lengths of 1, 4, and 10 cycles. The procedure was repeated outside the magnet using the PVDF hydrophone. In Fig. 7 the normalized pressure amplitude of each hydrophone is plotted as a function of distance indicating strong correlation between the waveforms, although a systematic error of approximately 20% is observed between the coil measurements and the PVDF hydrophone data. In addition to the uncertainty in the PVDF hydrophone calibration, error is introduced in part by the approximation presented in (4). The differing spatial characteristics of the EM hydrophone and the PVDF hydrophone may also account for some small differences in these axial scans. At the transducer resonant frequency of 0.748 MHz, the calibration constant exhibits an 11% divergence from the exact three-layer system solution calculated using (4). Additionally, curvature of the wire layer introduces error into our calculation, which is based on continuous layers. It is evident from (6) that sensitivity to the wire parameters is significantly reduced for thinner wire. Under the current experimental parameters but using a wire diameter below 50 μm, the calibration factor α would vary by less than 10% for any thickness value. Any generation of surface acoustic waves should not contribute significantly to the overall error as the small angle of incidence of the ultrasound upon the plexiglass centered coil suggests that this mode conversion is negligible [7].

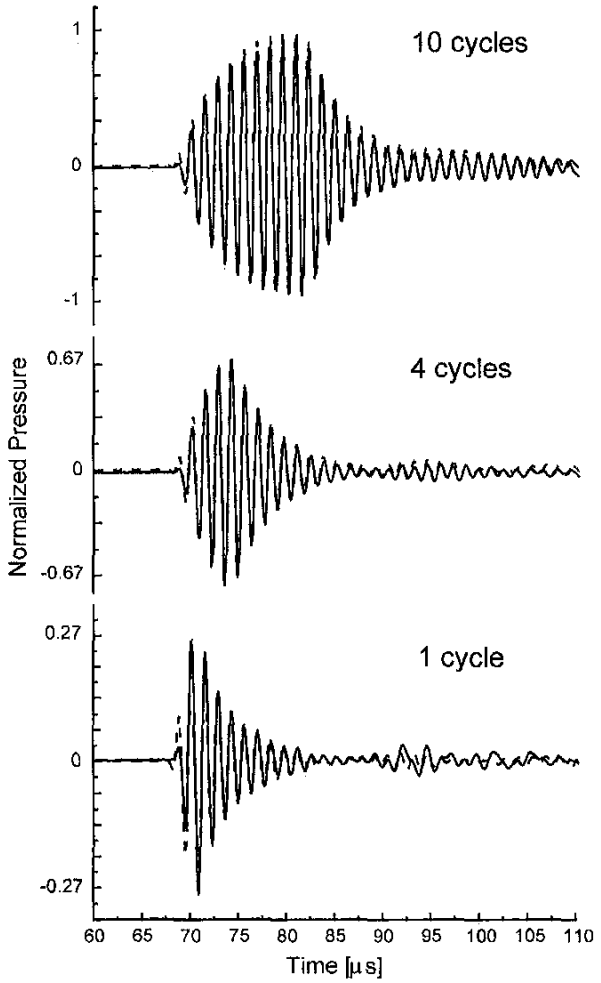

Fig. 6. Time traces of the normalized pressure field acquired using the 6-turn hydrophone (solid) and the PVDF hydrophone (dashed). Results obtained for burst lengths of 1, 4, and 10 cycles are shown. The 6-turn hydrophone is normalized over 185 kPa, and the PVDF hydrophone is normalized over 150 kPa. The distance of the detectors from the surface of the transducer was 100 mm. Measurements with EM hydrophone were carried out at 1.5 T.

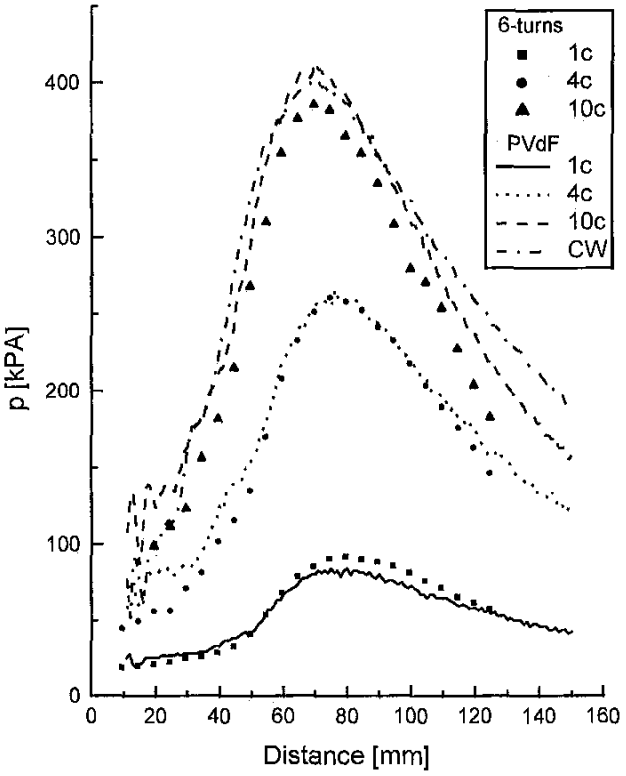

Fig. 7. Axial scans of the maximum peak-to-peak pressure amplitude. Scans obtained with the PVDF hydrophone (lines) and the 6-turn hydrophone (symbols) at magnetic field of 1.5 T. Burst lengths are indicated in the legends. The error in the measurement of distance inside the magnet is ±1 mm.

The hydrophone is sensitive to the acoustic velocity vector, which in some respect makes the model a paraxial approximation. Divergence, or convergence of beams far from the acoustic axis, would be sensitive only to the component of the velocity parallel to the acoustic axis. This is not problematic for most fields, including the measurement of fields near the focus of convergent beams, which have vectors approximately parallel to the axis of propagation. Heating of the coil core by focused ultrasound beams at very high power possibly could affect measurements due to expansion and alteration of the sound speed, although such effects on the hydrophone have not been studied at this time.

Similar measurements were conducted in field of 4.7 T using the same experimental setup. Signal shapes were similar to those obtained in the lower field but with proportionally higher intensities. A comparison between axial scans obtained at the two different fields, is given in Fig. 8. The ratio between left and the right scales in the figure is set to the inverse ratio of the two fields, i.e., 4.7/1.5=3.13. The small deviations between the two lines are mainly due to the experimental errors in positioning the hydrophone.

B. Wireless Reception

In order to demonstrate the feasibility of performing wireless measurements, a series of experiments was conducted using RF-pickup coils. The spatial sensitivity of the coils was determined using another RF test loop. The results are shown in Fig. 9. In the space between the two coils, the sensitivity reached its maximum and was relatively homogeneous (±5%) over the volume of about 88 cc. For the ultrasound measurements, an aluminum foil (d = 25 mm, thickness 20 μm) was used in place of the hydrophone coil. The time trace recorded over a four cycle burst length is shown in Fig. 10(a) and compared with a PVDF hydrophone measurement in Fig. 10(b). Because the wireless receiving coils are not calibrated, the measurements are presented in terms of the received voltage. Differences between the four cycle signals of Figs. 6(b) and 10 can be attributed to the three order of magnitude drop in the received signal in addition to small alignment errors.

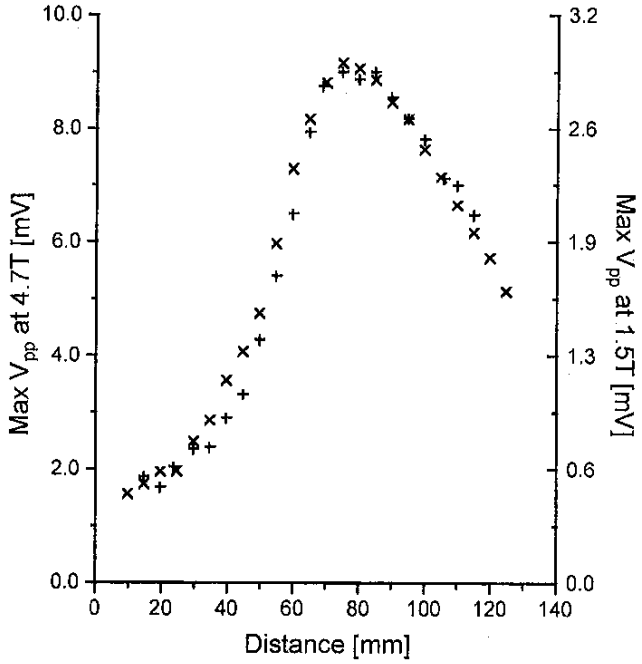

Fig. 8. A comparison between axial scans obtained at magnetic field strengths of 4.7 T (+) and 1.5 T (×). The two scales are set to the proportion ration of 4.7/1.5 between the two fields.

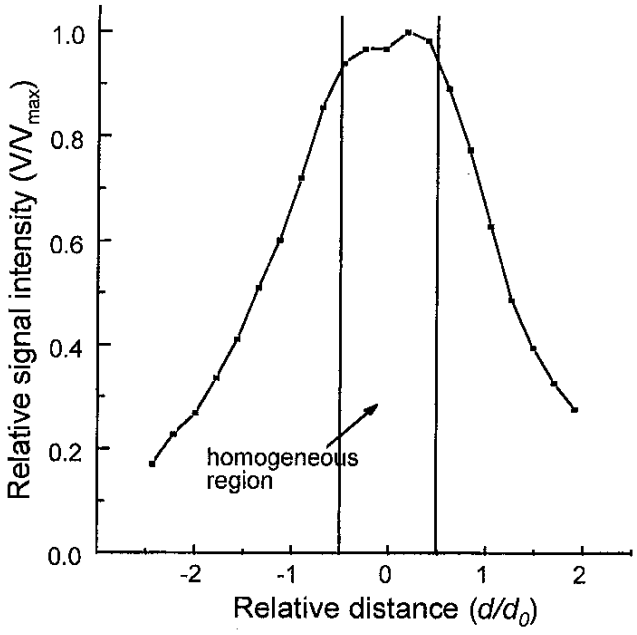

Fig. 9. A sensitivity profile for the horizontal pair of pickup coils. The sensitivity is highest and relatively uniform (±5%) in the region between the coils and drops sharply as r^{-1} with distance. The distance between the two coils is $d_0 = 23$ mm.

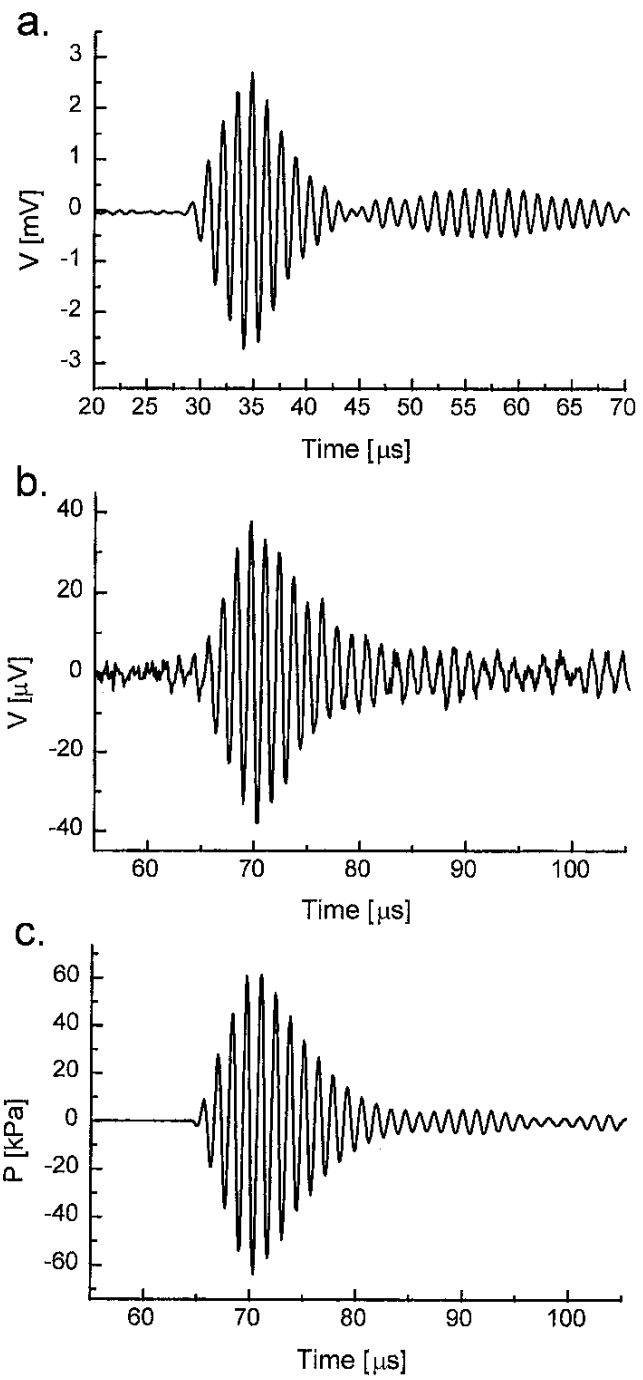

Fig. 10. Time traces obtained using RF pickup coils. The active elements were (a) A circular ($d = 25$ mm) aluminum foil measured at a magnetic field of 1.5 T. (b) A rectangular 3.3 mm∗1.4 mm aluminum foil recorded at 4.7 T. This time trace is the result of the subtraction after a 180° rotation of the chamber relative to the magnetic field. (c) The signal recorded using the PVDF hydrophone. All measurements were obtained with an input voltage of 30 mV peak-to-peak prior to the 55 dB RF amplifier and a burst length of four cycles.

Local measurements of the ultrasonic pressure field were carried out using a rectangular piece of aluminum foil of much smaller size (3.3 mm × 1.4 mm).The long axis of the element was placed perpendicular to both the magnetic field and the sonication axis [Fig. 3(b)]. To increase the signal strength, the measurement was taken in the 4.7 T magnet. The input voltage was similar to that used for the coil hydrophone measurements, but the observed signal intensities were about three orders of magnitude lower. Moreover, coupling noise, particularly at shorter distances, distorted the signal. To suppress the coupling, two consecutive time traces were recorded. After an initial measurement, the chamber was rotated by 180° relative to the magnetic field, and the data again was recorded. By (2), the emf of these data sets should differ in sign, and coupling noise is invariant to the rotation. The final signal shown in Fig. 10(c) is obtained by subtracting the two time traces. This method was successfully used to allow the measurement of the time trace signal from the small strip of aluminum foil. Apart from the inconvenience in repeating each measurement twice, the reduction in the noise level is limited to the dynamic range of the oscilloscope.

V. Conclusions

Our results show that electromagnetic (EM) hydrophones are capable of assessing the ultrasonic field parameters in the presence of static uniform magnetic fields. A systematic error of approximately 20% was observed between measurements taken independently with the EM hydrophone and with a PVDF hydrophone using 0.748 MHz transducer in a 1.5 T magnet. Excellent agreement was observed between the pressure waveforms of the hydrophones. However, unlike PVDF hydrophones, EM hydrophones offer the advantages of durability and simple assembly. These hydrophones are inexpensive when used in conjunction with a preexisting magnetic source and can exhibit a broad frequency response.

The emf generated in the EM hydrophone is found to be proportional to the amplitude of the ultrasonic pressure. This expected and yet remarkable linearity with the pressure amplitude was demonstrated over four orders of magnitude. Similarly, the expected linear dependency of the signal intensity with the strength of the magnetic field was demonstrated in 1.5 T and 4.7 T. These results agree with those reported in inhomogeneous fields [2], [3].

Results suggest that electromagnetic hydrophones are suitable for calibration as well as quality assurance of ultrasound devices operating in the vicinity of high magnetic fields. In addition, we demonstrate the potential for wireless acoustic field detection using RF pick-up coils, opening the possibility of future use as embedded receivers within test materials or in vivo tissues. Currently, the main obstacle in applying this method in vivo is the signal-to-noise ratio that limits the size of the conducting element. However, it is reasonable to believe that a better detection scheme will be available in the future, allowing substantial reduction in the element size.

References

[1] R. T. Beyer and S. V. Letcher, *Physical Ultrasonics*. New York: Academic, 1969, Chap. 10.

[2] L. Filipczynski, "Absolute measurements of particle velocity, displacement or intensity of ultrasonic pulses in liquids and solids," *Acoustica*, vol. 61, pp. 173–180, 1969.

[3] J. Etienne, L. Filipczynski, T. Kujawska, and B. Zienkiewicz, "Electromagnetic hydrophone for pressure determination of shock wave pulses," *Ultrason. Med. Biol.*, vol. 23, pp. 747–754, 1997.

[4] K. Hynynen, A. Darkazanli, E. Unger, and J. F. Schenck, "MRI-guided noninvasive ultrasound surgery," *Med. Phys.*, vol. 20, pp. 107–115, 1993.

[5] L. E. Kinsler, A. R. Frey, A. B. Coppens, and J. V. Sanders, *Fundamentals of Acoustics*. New York: Wiley, 1982, pp. 124–131.

[6] P.N.T. Wells, *Biomedical Ultrasonics*. New York: Academic, 1977, pp. 14.

[7] B. A. Herman and G. R. Harris, "Calibration of miniature ultrasonic receivers using a planar scanning technique," *J. Acoust. Soc. Amer.*, vol. 72, pp. 1357–1362, 1982.

[8] W. G. Mayer, "Energy partition of ultrasonic waves at flat boundaries," *Ultrasonics*, vol. 3, pp. 62–68, 1965.